The Crop Journal 12 (2024) 836–844

Contents lists available at ScienceDirect

The Crop Journal

journal homepage: www.keaipublishing.com/en/journals/the-crop-journal/

Natural variation in maize gene *ZmSBR1* confers seedling resistance to *Fusarium verticillioides*

Yunxia Song [a], Peipei Ma [b], Jingyang Gao [a], Chaopei Dong [a], Zhao Wang [a], Yifan Luan [a], Jiafa Chen [b], Doudou Sun [b], Pei Jing [b], Xuecai Zhang [c], Weibin Song [d], Zijian Zhou [b,*], Jianyu Wu [a,b,*]

[a] College of Agronomy, Henan Agricultural University, Zhengzhou 450002, Henan, China
[b] College of Life Sciences, Henan Agricultural University, Zhengzhou 450002, Henan, China
[c] Global Maize Program, International Maize and Wheat Improvement Center (CIMMYT), Apdo 6-641, 06600 Mexico, DF, Mexico
[d] National Maize Improvement Center, Department of Plant Genetics and Breeding, China Agricultural University, Beijing 100193, China

ARTICLE INFO

Article history:
Received 29 January 2024
Revised 3 April 2024
Accepted 16 May 2024
Available online 27 May 2024

Keywords:
Seedling blight
Stalk rot
Multiple disease resistance

ABSTRACT

Maize seedling blight caused by *Fusarium verticillioides* is a widely occurring maize disease, but the genetics and mechanisms of resistance are not well understood. In this study, GWAS performed by MLM and 3VmrMLM identified 40 and 20 QTNs, associated with seedling blight resistance. These methods identified 49 and 36 genes, respectively. Functional verification of candidate gene *ZmSBR1* identified by both methods showed that the resistance of a mutant line to seedling blight decreased by 0.37 grade points after inoculation with *F. verticillioides*, compared with the WT. The length of the stem rot lesion caused by *F. verticillioides* increased by 86% in mutant seedlings, and the relative length of the adult plant stalk rot increased by 35% in mutant plants compared to the wild type after inoculation with *Fusarium graminearum*. Transcriptome analysis showed that expression of defense-related genes after inoculation was down-regulated in the mutant compared to the wild type, synthesis of secondary metabolites associated with resistance was reduced, and the immune response triggered by PAMP decreased, resulting in decreased resistance of mutant maize seedlings. Candidate gene association analysis showed that most maize inbred lines carried the susceptible haplotype. A functional PCR marker was developed. The results demonstrated that *ZmSBR1* conferred resistance to multiple Fusarium diseases at the seedling and adult growth stages and had important application value in breeding.

1. Introduction

Maize is a widely cultivated food, feed and industrial crop. However, maize production is often affected by disease. *F. verticillioides* is a major maize pathogen [1] that can infect maize throughout the entire growth cycle. The fungus can be seed-borne, soil-borne or air-borne to cause disease variously known as maize seedling blight, stalk rot, ear rot, and seed rot [2–8]. It can systematically colonize the kernels in infected mature plants causing seedling blight at germination or infects newly emerging seedlings from infected trash, triggering a new cycle of infection [9].

Maize seedling blight occurs worldwide and causes severe yield losses when it occurs [10]. The incidence of maize seedling blight has increased in China in recent years due to continuous cropping or crop rotation systems that favor pathogen survival with the consequence that seedling blight has become a leading maize disease in that country. After infection with *F. verticillioides*, maize seedlings show reduced root weight, leaf lesions, leaf abnormalities, growth retardation, and even death, with consequent effects on yield [11–13]. Although fungicides and biocontrol bacteria provide some control [14], the best solution is genetic resistance. For this to be successful, sources of resistance are needed along with knowledge of the basis of resistance. Currently, most of the research on diseases caused by *F. verticillioides* infection is focused on stalk rot and kernel infection, and studies on the genetics of resistance at the seedling stage have been largely neglected. It is also important to identify resistance genes and to screen high-quality germplasm resources for resistance at the seedling.

Research on maize seedling blight has made some progress in recent years. Stagnati et al. [6] identified 4 quantitative trait nucleotides (QTNs) for disease severity on chromosomes 3 and 4 by genome-wide association analysis (GWAS). Most of the genes were

* Corresponding authors.
E-mail addresses: zhouzijian19900601@163.com (Z. Zhou), wujianyu40@126.com (J. Wu).

https://doi.org/10.1016/j.cj.2024.05.003

transcription factors, chitinase, and cytochrome P450 involved in general plant defense against pathogens [6]. Septiani et al. [15] identified three QTL for Fusarium seedling rot (FSR) on chromosomes 4 and 5 in a MAGIC population. Transcriptomics and sequencing information were also used to identify candidate genes. Seedlings of a *UFMulox4* mutant lacking *ZmLOX4* showed increased susceptibility to *F. verticillioides* [16]. *ZmLOX12* played a key role in defense against *F. verticillioides* in diverse maize tissues [17].

Typical symptoms for maize seedling blight are leaves at the base of the plant gradually becoming yellow, primary roots usually discolored or rotted, retarded growth, and finally wilting and plant death. Seedling blight is mainly caused by infection of the root [18]. Following artificial inoculation of the stem at the seedling stage there is gradual browning around the inoculation site followed by expansion with hyphal spread [19]. As stem rot progresses, the plant may show wilting or breaks from the stem inoculation site. The typical symptoms of maize stalk rot appear at late milk to wax ripeness stage. Stalk rot not only causes rotting of the stem base, but also hinders the transport of nutrients [20,21]. Most stalk rot infection occurs at the seedling stage and the pathogen continues to spread systematically as the plant grows. With severe infection, the pathogen enters the maize ears and causes ear rot [22]. It is critical to prevent *F. verticillioides* infection at the seedling stage as there are limited control measures following initial infection. The occurrence of maize seedling blight can also lead to the occurrence of sever disease symptoms such as stalk rot and ear rot, suggesting that it is important to study the mechanism of resistance to seedling blight.

To our knowledge, there are very few reports of cloning and further functional verification of natural variant genes associated with maize seedling blight resistance using natural population. In our research, the resistance gene *ZmSBR1* was identified by GWAS based on the establishment of a quantitative resistance identification index system. Functional verification was performed by artificial inoculation of the mutant. In addition, transcriptome data were used to investigate the resistance mechanism of *ZmSBR1*. We also identified the optimum haplotype of *ZmSBR1* and developed a functional molecular marker for use in breeding for resistance. It is helpful to identify some key maize lines in China and the analysis of pedigree relationships provides the foundation for formulating breeding strategies for disease resistance.

2. Materials and methods

2.1. Plant and pathogen materials

A collection of 219 diverse inbred lines for the association-mapping panel for genome-wide association analysis of maize seedling blight included the heterotic populations Tangsipingtou and Reid, and some tropical lines from the International Maize and Wheat Improvement Center (CIMMYT). An EMS-induced early termination mutant of inbred line B73 was purchased from the mutant website (http://maizeems.qlnu.edu.cn/). The *F. verticillioides* strain was isolated from naturally infected maize kernels collected at Zhengzhou by using the single-spore isolation method [2]. Spores were collected after the fungus was cultured in sterilized maize kernel medium at 28 °C in darkness for 5–7 d. The spores were eluted from the medium by adding sterile water, and filtered with eight layers of sterile gauze to collect the spores and then adjusted to 5×10^7 spores mL^{-1} with sterile water.

2.2. Artificial inoculation and phenotypic evaluation

Maize seedling blight response was assessed following artificial inoculation. Healthy maize seeds were sown in 50-hole trays filled with soil mix and cultured in an incubator at 28 °C with 16 h light and 8 h darkness for 7–8 d to the two–three leaf stage. Plants of uniform size were selected and gently washed to remove substrate from the root surface. The GWAS population was set up in three replications and three plants per line were inoculated. For the mutant and wild type lines, we inoculated 32 and 51 plants, respectively, to investigate the response to seedling blight. All plants were inoculated by placing the roots of each plant in 10 mL of spore suspension and transferring them to a growth chamber at 28 °C and a 16 h light/8 h darkness photoperiod. Infection severity was recorded after 5 d. We used a 6-score phenotyping scale with 0 being the most resistant and 5 being dead (Table S1). The data were analyzed as mean scores per replicate.

For the evaluation of maize seedling response to stalk rot, nine healthy maize seedlings grown in 10 cm × 10 cm pots in a 28 °C incubator at, with 16 h light/ and 8 h darkness for about 8 d (two–three leaves). Plants of similar size were selected for inoculation; including 72 wild-type plants and 82 mutant plants. A 1 mL sterile syringe was used to inject 100 μL of *F. verticillioides* spore suspension (2×10^8 spores mL^{-1}) into the middle of each stalk [19]. The phenotypic evaluation was made 5 d post inoculation. Fungal content was quantified using the method described by Ma et al. [20].

Evaluation of adult plants to stalk rot caused by *F. verticillioides* was carried out according to the method described by Ma et al. [20] with some modifications. Drill holes in the penultimate stem nodes of maize plants 15 d post pollination were injected with 200 μL of *F. verticillioides* spore suspension (5×10^7 spores mL^{-1}) [5]; 15 wild type and 20 mutant plants were inoculated, respectively. The toothpick method [23,24] was used to inoculate adult plants with *Fusarium graminearum* for assessment of stalk caused by that species. Each plant was then inoculated by inserting one toothpick into the penultimate node at 15 d post pollination, with 11 wild type and 44 mutant plants being inoculated.

2.3. Phenotypic data analysis

The best linear unbiased predictions (BLUP) of phenotypic data from the three replicates were calculated using IciMapping4.1.0.0 (http://www.isbreeding.net, accessed on January 13, 2024). Broad sense heritability (H^2) was calculated using the formula (1).

$$H^2 = \frac{\sigma_g^2}{\sigma_g^2 + \sigma_{ge}^2/n + \sigma_e^2/nr} \quad (1)$$

where σ_g^2, σ_{ge}^2, and σ_e^2 represent the genotypic, genotype × environment, and residual error variances, respectively; n is the number of environments; and r represents replications as a random effect, respectively [25]. Normality tests for the association mapping panel were carried out using the Shapiro-Wilk test in SAS. The BLUP values were used in GWAS.

2.4. Genome-wide association analysis

To explore the genetic basis of resistance to seedling blight, 219 inbred lines and 292,147 SNPs were used to performed genome-wide association analysis. We evaluated the phenotype of the GWAS population after artificial inoculation according to the 0–5 disease severity grading system (Fig. S1). Genotypes of the diversity panel were obtained by the genotyping-by-sequencing (GBS) method [26]. As described previously [27], the GWAS population was divided into three subgroups, where subgroup 1 contained the most diverse 180 tropical germplasm accessions from CIMMYT [2]. A total 955,650 SNPs were filtered to remove those with missing values of more than 0.25 and minor allele frequency (MAF) less than 0.05 leaving 292,147 for further analysis. Principal compo-

nent (PCA), kinship matrix (K), and linkage disequilibrium (LD) analyses for each pair of SNPs were conducted by using TASSEL 5.0 software [27]. The GWAS analysis was performed using the MLM + K + PCA mode in TASSEL 5.0. The genome-wide significance threshold ($P < 10^{-4}$) for identification of QTNs was based on previous studies [27–29]. The 3VmrMLM method [30] was also used for GWAS and ⅢVmrMLM software [31] was used to detect QTNs associated with resistance to *F. verticillioides* at the seedling stage. The critical *P*-value was set as 1.0/m for declaration of QTNs, where m was the number of markers. Candidate gene information was deduced from the physical positions of significant QTNs in the MaizeGDB database (https://www.maizegdb.org/, accessed on January 13, 2024). Genomic information, gene model, and possible functional annotation of candidate genes were based on B73 RefGen_v2. We conducted three batches of experiments, every batch consisting of three replicates to perform independent GWAS. We treated each group of experiments as a separate environment for subsequent heritability analysis.

2.5. Candidate gene association analysis and functional marker development

The GLM model in TASSEL 5.0 was used to perform the candidate gene association analysis of *ZmSBR1*; 354 SNPs in the promoter and genome region of *ZmSBR1* were identified from the 35× resequencing results of 178 maize inbred lines. After filtering and polymorphism analysis, 84 high quality SNPs were used for candidate gene association analysis, and the results were visualized using the R package IntAssoPlot [32]. A functional indel marker was validated using 102 inbred lines from the GWAS population. PCR and agarose gels electrophoresis were used to ascertain the type of insertion and deletion markers by electrophoretic band size. The significance test was then conducted by combining the corresponding phenotypes and genotypes.

2.6. Subcellular localization

To determine the subcellular localization of *ZmSBR1*, the full-length CDS was cloned into the pCAMBIA1302 plasmid driven by the 35S promoter by homologous recombination (SE Seamless Cloning and Assembly Kit, ZOMANBIO). The fusion construct was transformed into *Escherichia coli* strain DH5α, and the plasmid was extracted using an E.Z.N.A Plasmid Mini Kit I (Omega). The plasmids were transferred into protoplasmic cells of maize hybrid Zhengdan 958. After dark treatment for 16 h, the cells were collected and imaged using a confocal microscope (Nikon A1R HD25). Fluorescence was examined under excitation wavelengths at 488 nm for GFP. Primers used in the study are listed in detail in Table S2.

2.7. RNA-seq analysis

Seedlings of B73, and homozygous positive and homozygous negative progeny of EMS mutants of B73 were inoculated with *F. verticillioides*. The roots were sampled at 0 h and 24 h after inoculation for RNA-seq. Three biological replicates were set up, each containing the roots from four seedlings. RNA-seq libraries were prepared according to the Illumina standard library preparation kit. Illumina NovaSeq 6000 (San Diego, CA, USA) was used as a platform for RNA-seq at BioMarker Technologies Co., Ltd. (Beijing). Qubit 3.0, combined with the Qsep400, was used for quality control checks on raw sequencing data. Clean reads were aligned to the B73 reference genome (RefGen_v4) and reference gene model dataset using HISAT2 software. Gene expression values were normalized as FPKM. A gene was assumed to be expressed only when the FPKM value was greater than zero in all three replicates. DEGs were identified by a false discovery rate threshold < 0.05 using the DESeq Software Package (bioconductor.org/, accessed on January 15, 2024) and annotated for assigning GO terms and metabolic pathways in the Kyoto Encyclopedia of Genes and Genomics (KEGG). Heat mapping of differentially expressed genes was performed using TBTools [33]. RNA-Seq analysis was performed using BMKCloud (www.biocloud.net, accessed on January 15, 2024).

3. Results

3.1. GWAS for seedling blight resistance

Frequency distribution analysis performed on seedling blight severity data for 219 inbred lines showed a normal distribution (Fig. S2). Average disease severity of individuals in the GWAS population ranged from 0 to 4.10 (Table S3). Inbred line CNW036 had the lowest disease grade of 0, and CNW030 had the highest grade of 4.10. Heritability (H^2) was 0.76 (Table S3), indicating that the phenotypic variation of the population was mainly genotypic.

According to the population structure analysis, single marker-based GWAS was performed using MLM, incorporating the first three principal components of the population structure and kinship (*K*) into the model. The quantile–quantile (QQ) plots showed that population structure was well controlled by PCA and *K* (Fig. S3). A total of 40 significant QTNs associated with maize seedling blight response were identified through combined analysis of the GWAS population with a threshold of 1.0×10^{-4}. These QTNs were located across all 10 chromosomes and explained 6.91% to 10.22% of the phenotypic variation. Linkage disequilibrium (LD) in the GWAS population measured in our previous study, showed a decay distance of 10–20 kb (R^2 = 0.1) at the single gene level [27]. Based on physical intervals of 20 kb surrounding significant QTNs we identified 49 genes (Fig. 1A; Table S4). We focused on three linked QTNs located on chromosome 8, S8_101960714, S8_101960790, and S8_101960795, with S8_101960714 being the most significantly associated QTN ($P = 8.03 \times 10^{-6}$).

We used the same PCA and kinship approach for 3VmrMLM analysis. Twenty QTNs significantly associated with seedling blight resistance were identified. These QTNs, located in chromosomes 1, 2, 3, 4, 5, 6, 7, 8, and 10, explained 0.76% to 8.53% of the phenotypic variation and corresponded to 36 genes (Fig. 1B; Table S5). The significant QTN S8_101960714 was again identified ($P = 2.09 \times 10^{-6}$). The LD interval of QTN S8_101960714 was 82 bp, with only *GRMZM2G149808* present in the block (Fig. 1D). We named *GRMZM2G149808* as *ZmSBR1* (*seedling blight resistance 1*) and focused on it in further studies (Fig. 1).

3.2. ZmSBR1 regulates the resistance of maize seedling to F. verticillioides

To determine its subcellular localization, we fused full-length ZmSBR1 to the N terminus of the enhanced green fluorescent protein (eGFP). Transient expression of the fusion protein in maize leaf protoplasts revealed its location in the nucleus (Fig. S4). Phylogenetic tree analysis revealed that *ZmSBR1* was highly homologous to *Zm00001d038258* on chromosome 6, indicating that the gene might have multiple copies (Fig. 2A). Domain prediction (SMART: Main page (https://smart.embl-heidelberg.de/)) indicated that *ZmSBR1* contained a SAP30_sin3_bdg domain, and may have a role in histone deacetylation. To determine the role of *ZmSBR1* in maize-fungus interaction we used the B73 mutant line (MEMD database: mutant ID: EMS3-08154b) [34]) carrying *zmsbr1*. Compared to the B73 reference genome, the *zmsbr1* allele contained a G/A substitution in the third exon of *ZmSBR1* that caused premature termination of translation at Trp163 in the SAP30_Sin3_bdg

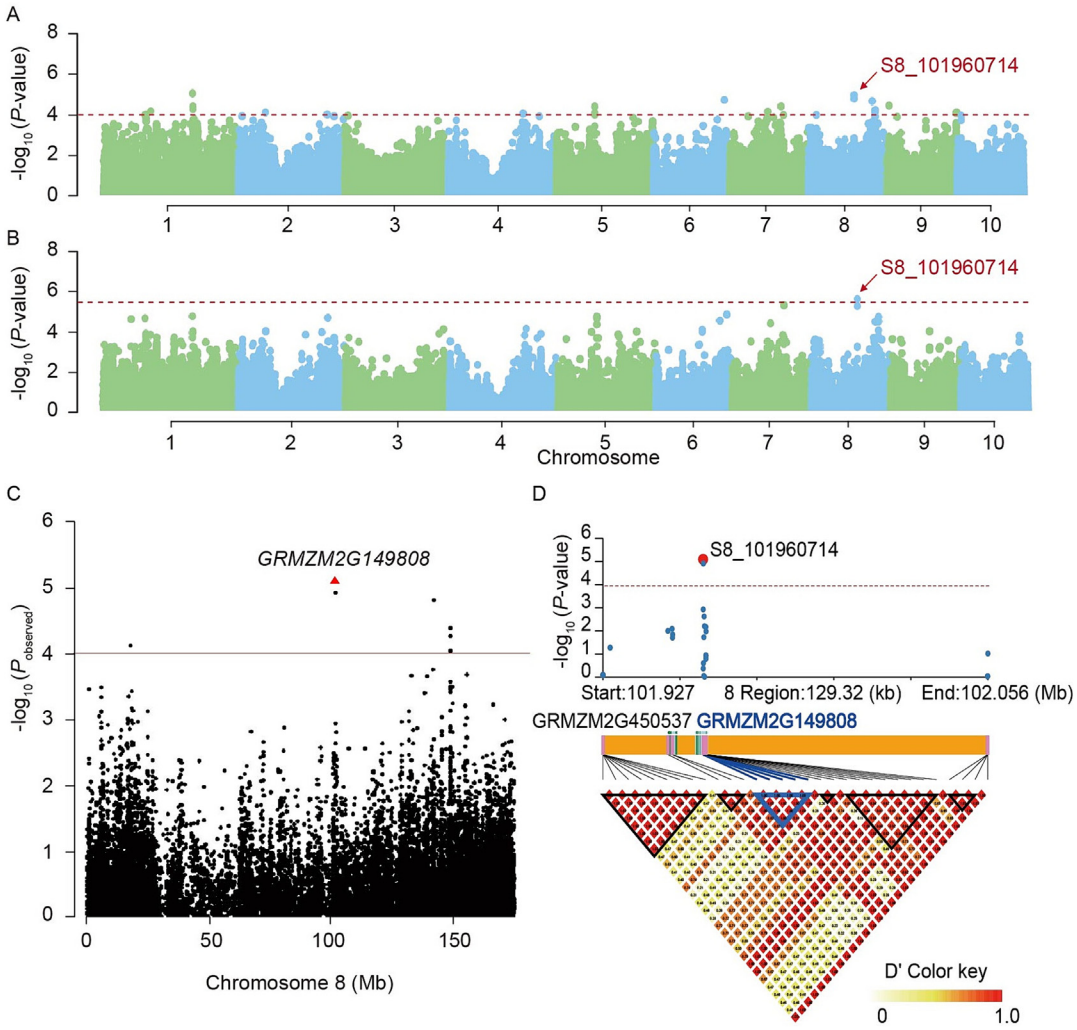

Fig. 1. Genome-wide association study (GWAS) on seedling response to *F. verticillioides*. (A) Manhattan plot of GWAS for maize seedling blight grades by MLM. Plots above the red line show genome-wide significance with a moderately stringent threshold ($P = 1.0 \times 10^{-4}$). QTN S8_101960714 is shown with a red arrow. (B) Manhattan plot of QTNs identified by 3VmrMLM. QTN S8_101960714 is shown with a red arrow. The horizontal axis shows the physical positions across the ten chromosomes. Plots above the red arbitrary line show the genome-wide significance with a threshold of $P = 3.42 \times 10^{-6}$. (C) Regional Manhattan plot of the *ZmSBR1* genomic region on chromosome 8. The lead QTN is shown by a red diamond. (D) Linkage disequilibrium analysis of QTN S8_101960714. The red dot indicates S8_101960714. There are six blocks in the LD diagram. The block corresponding to QTN S8_101960714 is shown in blue. This block is an independent block and contains only one gene, *GRMZM2G149808*.

domain (designated *zmsbr1*$^{W163^*}$) (Fig. 2B, C). Heterozygous mutant plants were self-crossed to obtain homozygous positive (*zmsbr1 lines*) and homozygous negative (*ZmSBR1 lines*) progeny for seedling inoculation and phenotyping.

Compared with the wild type, mutant seedlings were taller and had longer roots and stem length (Fig. 2D–G). Following inoculation with *F. verticillioides*, the first leaf began to lose greenness from the tip, and gradually turned yellow and then, brown. The first leaf of the *zmsbr1* mutant line was completely dried up, the entire second leaf turned yellow, and even the tip of the leaf was dry at 6 d post inoculation, indicating a faster response. Compared to the *ZmSBR1* line, the disease rating of the *zmsbr1* mutant line was increased by 0.37 grade points (Fig. 2H, I). DAB staining of the roots of inoculated seedlings showed hydrogen peroxide accumulation at the infection site with the degree of necrosis in the mutant lines being more severe than in the WT (Fig. 2H). In addition to the roots, we also identified the resistance of isolated leaves to *F. verticillioides*. After leaf inoculation a waterlogged appearance became evident and was more severe in leaves of the mutant. The growth of mycelia in mutant seedling leaves was significantly more than in the WT. Fungus content in isolated leaves of mutant seedlings was 1.9-fold that of the WT (Fig. 2J, K). Therefore, the resistance in both roots and leaves of the mutant to *F. verticillioides* was significantly decreased relative to the WT. These results indicate that *ZmSBR1* positively regulates the resistance of maize seedlings to *F. verticillioides*.

3.3. ZmSBR1 confers maize resistance to stalk rot

After stem inoculation with *F. verticillioides*, the surface around the inoculation site turned brown, followed by rotting and expansion of the infected area. When the stem rot was severe enough, the plant collapsed. The *zmsbr1* mutant plants exhibited higher susceptibility with an 86% increase in stalk rot length compared to the WT. DAB staining confirmed that the mutant was less resistant than the WT (Fig. 3A–C). During development of stem rot, we observed that seedling leaves also became blighted. The severity of seedling blight caused by stalk rot at six days post inoculation was

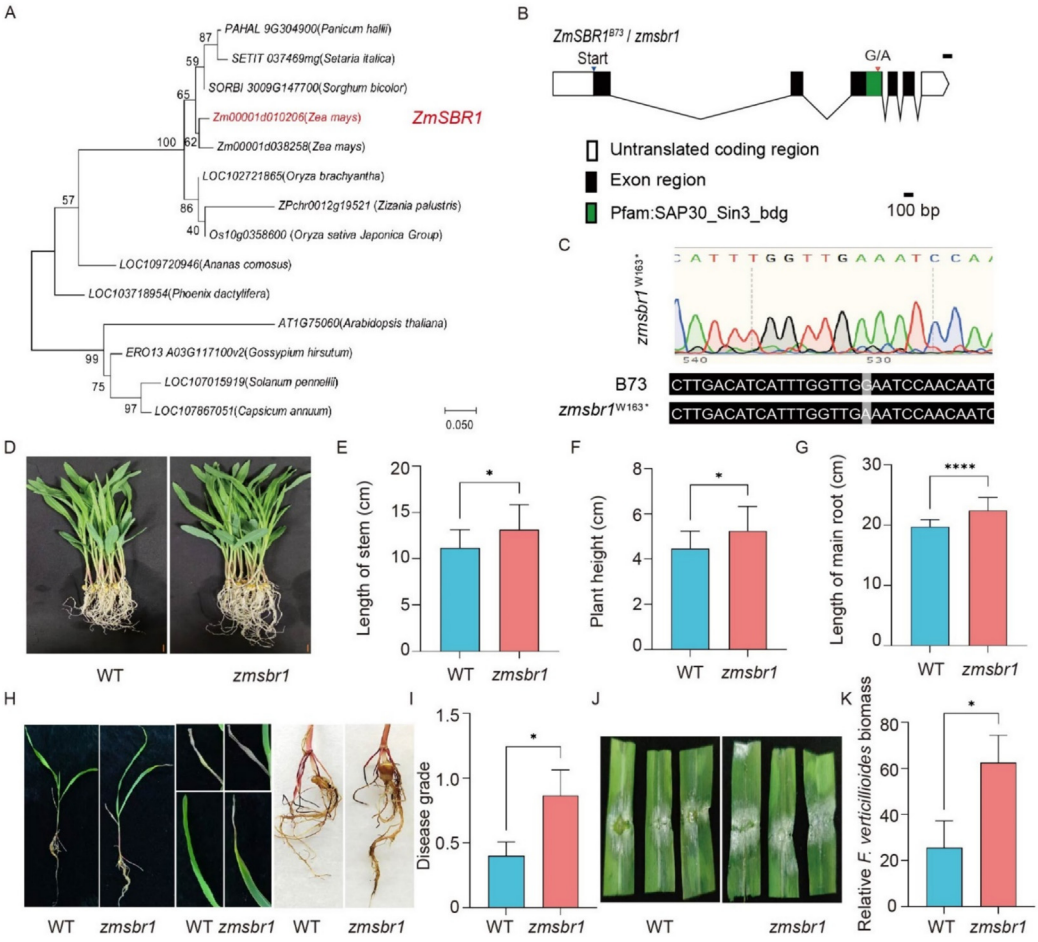

Fig. 2. Function of *ZmSBR1* in maize seedling blight resistance. (A) Phylogenetic tree of *ZmSBR1* homologues in different species. The sequences of *ZmSBR1* homologues were obtained from the NCBI database, and phylogenetic analysis was performed using MEGA 7.0. (B) Schematic diagram of *ZmSBR1*^{B73}/*zmsbr1*. Protein-coding regions are indicated in black bars. The SPA30_Sin3_bdg domain is indicated by a green bar. UTRs are indicated in white bars. Red inverted triangle indicates the position of the base change from G to A. (C) Verification of the mutant allele by PCR-based sequencing. The mutation of the base from G to A in the mutant line caused premature termination of protein translation. (D–G) Plant height and main root length of *zmsbr1*mutant plants is increased. Scale bar, 2 cm. (H–I) Phenotypes of mutant (*zmsbr1*) and wild-type plants (WT). Mutant (n = 32) and WT (n = 51) seedlings at the 2–3-leaf stage were inoculated with *F. verticillioides*, and the roots were stained with DAB. The phenotypic evaluation was performed 5 d post inoculation. (J) Phenotypes of inoculated mutant and isolated WT leaves. (K) Quantification of internally *F. verticillioides* levels in the isolated leaves by quantitative PCR. Maize *Ef1a* was used as the internal control. Statistical significance was determined by a two-tailed t-test (P = 0.0226); * indicates a significant difference at $P < 0.05$ (Two-sided Student's t-test).

increased by 81% compared to the wild type (Fig. 3E, F). Fungal biomass of *F. verticillioides* accumulation in stems and roots of mutant plants was 2 and 31-fold that of WT, respectively, which was significantly higher than that of WT (Fig. 3D, G, H). The above results indicated that *ZmSBR1* also positively regulates seedling stalk rot resistance to *F. verticillioides*.

The effect of *ZmSBR1* on stalk rot resistance in adult maize was investigated by inoculating the penultimate stalk node of the EMS mutant lines with *F. verticillioides* spore suspension 15 d after pollination. At 20 d post inoculation, rotting phenotype was present near the inoculation site when the stem was cut longitudinally, but the rot was mostly confined to the inoculated node and did not break through the stalk node. We then measured the relative rot length of the stalk and found no significant difference between the mutant and WT plants (Fig. 3I, J). Similar phenotypes were observed after inoculation with *F. graminearum*, the dominant fungal species involved in stalk rot; the mutant plants were more susceptible to stalk rot than the WT, with a 35% increase in relative stalk rot length (Fig. 3K, L). These results suggested that *ZmSBR1* played a positive regulatory role in the resistance of adult plants to stalk rot caused by *F. graminearum*.

3.4. Loss-of-function of ZmSBR1 reduces PAMP-triggered immunity and synthesis of disease resistance-associated secondary metabolites

Transcriptome analysis of ZmSBR1 and zmsbr1 lines and B73 was performed at 0 h and 24 h post inoculation. The principal component analysis is shown in Fig. S5. There were 5147 differentially expressed genes at 24 h post-inoculation (pi), of which 3042 were down-regulated and 2,105 were up-regulated in the zmsbr1 mutant. For the ZmSBR1 line, 2382 DEGs were down-regulated and 2015 DEGs up-regulated after inoculation. At 0 h, only 17 DEGs were detected between the ZmSBR1 and zmsbr1 lines. Compared with the ZmSBR1 line, the zmsbr1 line had 10 down-regulate, and 7 genes up-regulated genes. However, at 24 hpi, there were 315 DEGs, 35 up-regulated, and 280 down-regulated, compared with the ZmSBR1 line (Fig. S5B; Table S6). These DEGs were significantly enriched in the phenylpropanoid biosynthesis, flavonoid biosynthesis, flavone and flavonol biosynthesis, plant-pathogen interaction, ABC transporters, stilbenoid, diarylheptanoid and gingerol biosynthesis pathways (Fig. S5C). The different expression of genes in the plant-pathogen interaction pathway (KEGG pathway, KO: zma04626) showed that PAMP-triggered immunity-related

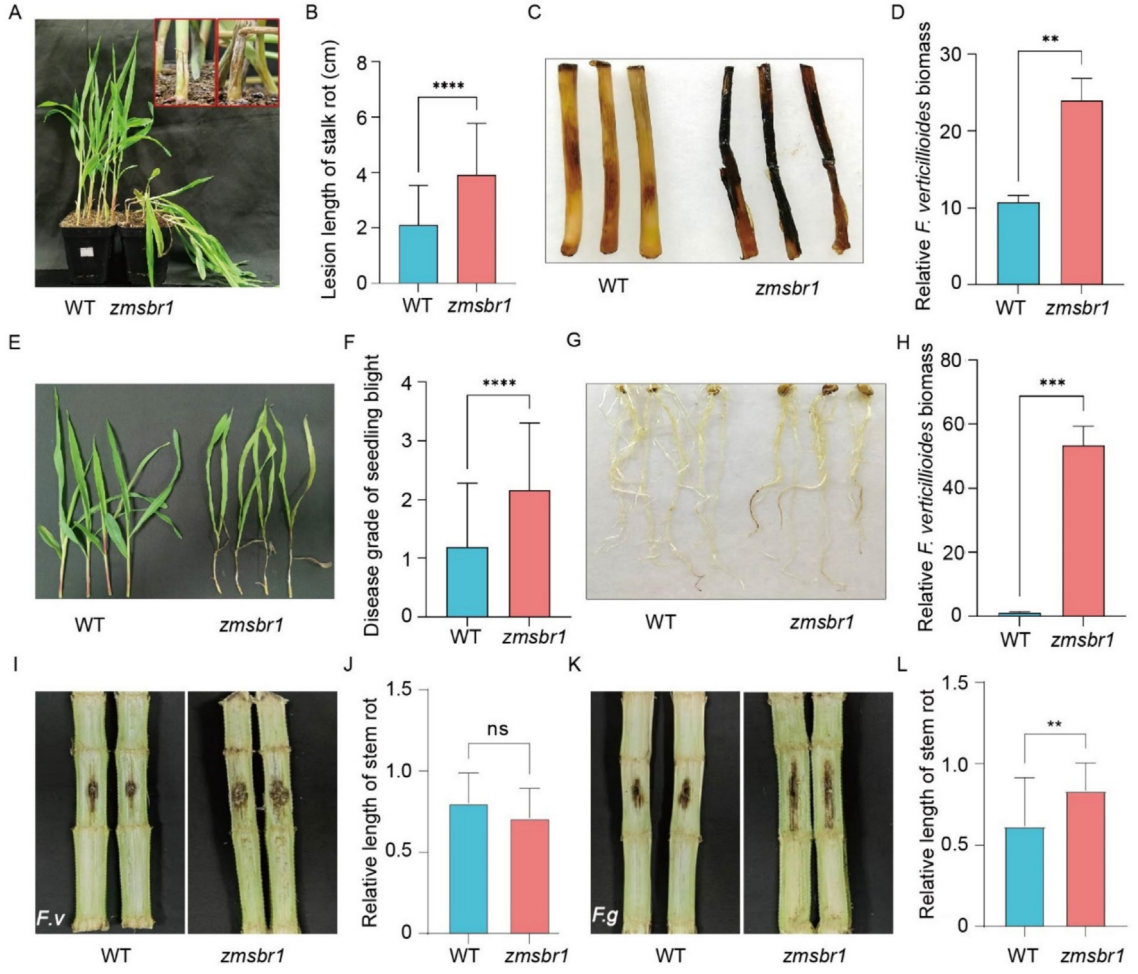

Fig. 3. *ZmSBR1* confers resistance to stalk rot. (A–B) *zmsbr1* mutant plants have decreased seedling stage resistance. Three-leaf seedlings of WT (n = 72) and the *zmsbr1* mutant (n = 82) lines were inoculated with *F. verticillioides*; phenotype (A), and disease severity (B) at 5 days post-inoculation. (C) DAB staining of stems near the inoculation site in stems of WT and *zmsbr1* mutant plants ($n \geq 3$), and contents of *F. verticillioides* (D). (E, F) Seedling blight phenotypes at 6 d post stem inoculation. (G, H) Root phenotypes and fungal biomass of WT and mutant plants following stem inoculation. Infected areas are brown. ($n \geq 3$). (I–L) Penultimate nodes of WT (n = 20) and *zmsbr1* mutant (n = 15) inoculated with *F. verticillioides* at 15 d post pollination and observed 20 d later. (J). Penultimate stalk nodes of WT (n = 11) and *zmsbr1* mutant (n = 44) plants inoculated with *F. graminearum* (*F. g*) at 15 d post pollination and observed 20 d later. (L). Statistical significance was determined by two-tailed t-tests; *, $P < 0.05$; **, $P < 0.01$; ***, $P < 0.001$; ****, $P < 0.0001$.

genes in the *zmsbr1* line were significantly down-regulated at 24 hpi compared with the *ZmSBR1* line. These results indicated that *ZmSBR1* regulated the resistance of maize seedlings to *F. verticillioides* by affecting plant-pathogen interaction and downstream secondary metabolite synthesis. We classified the DEGs into eight categories based on GO and CGO annotation information in the transcriptome data. They were related to cell wall synthesis, transcription factors, secondary metabolite synthesis, signal transduction, amino acid transport, inorganic ion transport, lipid transport, and metabolism and carbon transport (Fig. S6A, B; Table S6).

3.5. A functional marker for maize seedling blight based on ZmSBR1

Five significant SNPs of the gene with the most significant S8_104002262 were found through the candidate gene association analysis of *ZmSBR1* (Fig. 4A). The 178 maize inbred lines were classified into two haplotypes according to these SNPs. Statistical analysis of the phenotypes of the two haplotypes showed that haplotype 1 (CTTGA, n = 29) had significantly ($P = 5.38 \times 10^{-5}$) higher disease resistance than haplotype 2 (TCCAG, n = 148) (Fig. 4B; Table S7). The more resistant haplotype Hap1 was more frequent in the Reid group, and least frequent in the TSPT group (Fig. 4C). Therefore, the variation of these SNPs may serve as a functional marker for maize seedling blight resistance breeding.

Sequencing of 4 resistant and 4 susceptible inbred lines indicated that the latter had deletions in the intron of *ZmSBR1* (Figs. S7A, S8) as shown by the lower bands after PCR amplification and electrophoresis (Fig. S7B). The indel sites in 102 inbred lines were detected by PCR amplification. Phenotype statistics showed a significant difference in seedling blight resistance between inbred lines with intact and deletion fragment. Materials containing the fragment had an average disease rating of 1.463, whereas those with the deletion had an average disease rating of 2.017 (Fig. S7C). The indel marker was also used for pedigree and candidate gene association analysis of 102 inbred lines. Consistent with the results of SNP haplotype analysis, pedigree categorization showed that inbred lines from the TSPT group were more susceptible with most of the inbred lines carrying the susceptible

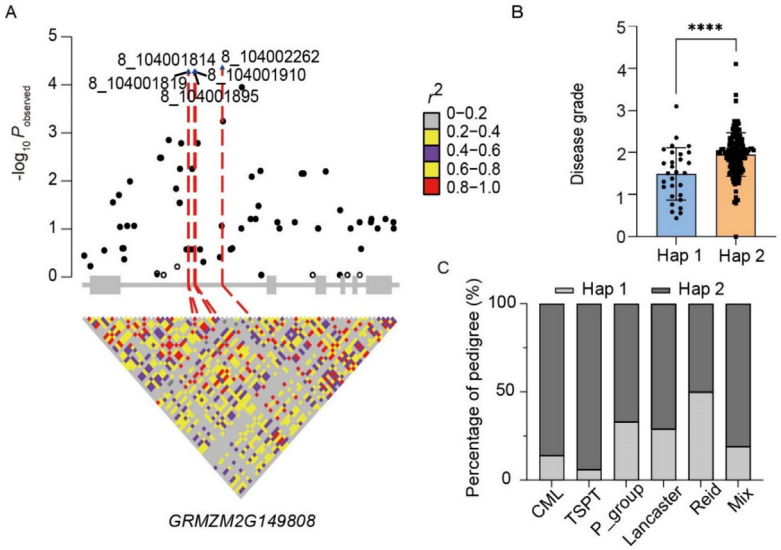

Fig. 4. Natural variation in *ZmSBR1* is significantly associated with maize seedling blight. (A) Association mapping and pairwise LD analysis of *ZmSBR1*. The lead and four highly significant QTNs are highlighted in blue. The QTNs showing strong LD with the lead QTN are connected to the pairwise LD diagram with line of red dashes. (B) Phenotypic differences between haplotypes (Hap 1, CTTGA; Hap 2, TCCAG) of *ZmSBR1*. Statistical significance was determined using a two-tailed *t*-test. ****, $P < 0.05$. The mean disease grade of each haplotype is shown (Hap 1, $n = 29$; Hap 2, $n = 134$). (C) Proportion of each haplotype in each major corn group.

genotype (Fig. S7D). Candidate gene association results showed a linkage disequilibrium between this indel marker and QTN marker S8_104002262 ($R^2 = 0.60$) (Fig. S7E).

4. Discussion

Maize seedling blight caused by *F. verticillioides* occurs at the early stage of maize plant growth and development, but the pathogen also causes systematic infection. However, as the first line of defense against the pathogen at the adult stage, seedling disease is often ignored by producers and researchers. In the summer of 2017, we investigated the incidence and severity of seedling blight of the GWAS population in the field at Xuchang and Zhengzhou in Henan province. Given the high incidence of seedling blight under natural environmental conditions and large effects of environment it was necessary to develop a laboratory system to study the genetics of seedling blight resistance. We found that some materials, such as CNW036, CNW057, CML27, and CML50, showed stable resistance to seedling blight under natural field conditions, with average disease severity grades of 0.50, 0.45, 0.23, and 0.81, respectively. With laboratory inoculation the corresponding disease grades of these materials were 0, 0.44, 0.56, and 0.67. Thus, for these materials, the resistance was basically consistent. Based on this identification system, we conducted a GWAS for maize seedling blight. In the GWAS population, normal distributions of seedling blight severity were observed (Fig. S2), and the heritability was 0.76 (Table S3), indicating that disease grade could be used as an index of disease response in genetic studies. In the GWAS, we identified several candidate genes, some of which encoded proteins often reported to be associated with plant disease resistance. Among them, *GRMZM2G478417*, *GRMZM2G148074* and *GRMZM2G171912* encoded bZIP transcription factors, which play an important role in plant growth and development and resistance to biological stress and biotic stress [35–38]; *GRMZM2G045270* and *GRMZM2G126928* encode ribosomal proteins, and some ribosomal proteins show antimicrobial peptide (AMP) activity [39]; and *GRMZM2G123094* encodes a C2H2-like zinc finger protein, which is involved in plant growth and environmental stress and regulates plant immunity [40–42]. Several of our candidate genes were reported to be associated with resistance to *F. verticillioides* in maize; for example, *GRMZM2G147966* was reported to be associated with ear rot resistance in a GWAS [43], and *GRMZM2G422576* was reported to be associated with resistance to fumonisin contamination [44]. Although some candidate genes were reported to be related to resistance to *F. verticillioides*, they have not been reported in genetic studies of maize seedling blight resistance or stalk rot resistance, possibly due to differences in population structure and resistance assessment methods [6,45].

In this study, we used the MLM and 3VmrMLM methods for GWAS. In the MLM method, we focused on three linked QTNs, S8_101960714, S8_101960790, and S8_101960795 located in chromosome 8, with S8_101960714 found to be the most significantly associated QTN ($P = 8.03 \times 10^{-6}$). With the 3VmrMLM method, we also identified QTN, S8_101960714 ($P = 2.09 \times 10^{-6}$) as the most significant. We focused on this QTN in subsequent studies. Based on the LD data from our previous study [27], we performed a search within a 20 kb interval surrounding these QTNs and identified two gene candidates, *GRMZM2G149808* and *GRMZM2G450537*. Candidate gene association analysis of these two genes indicated that *GRMZM2G450537* was not associated with seedling blight resistance (Fig. S9). LD analysis of QTN S8_101960714 showed that there was only one gene, namely *GRMZM2G149808* (*ZmSBR1*), in the block where the QTN was located. *ZmSBR1* contains a SAP30_Sin3_bdg domain, a histone deacetylase complex component conserved among eukaryotic organisms [46]. The combination of SAP30 and mSin3 can mediate transcriptional inhibition through histone deacetylase and can form a complex with HDAC to participate in the transcriptional regulation of the plant circadian rhythm, plant defense response, and cell death [47–53]. To our knowledge, the role of SAP30_Sin3_bdg in plant disease resistance has not been extensively reported. In this study, the decreased resistance of the *zmsbr1* mutant to maize seedling blight after inoculation with *F. verticillioides* suggested that *ZmSBR1* may positively regulate maize seedling resistance. The transcriptome results further indicated that *ZmSBR1* positive regulated maize resistance to seedling blight by promoting the expression of downstream resistance genes and

synthesis of secondary metabolites affecting disease response, and further activating the PTI pathway (Fig. S6C). These results suggest that secondary defense metabolites also play a crucial role in resistance to seedling blight. The current study demonstrates that resistance to Fusarium seedling blight in maize is complex and depends on a network of multiple defense pathways. In addition, loss-of-function of *ZmSBR1* showed decreased resistance to seedling stalk rot caused by *F. verticillioides* and adult stalk rot caused by *F. graminearum*. Inoculation of seedling stems with *F. verticillioides*, not only caused stem rotting but also leaf symptoms like seedling blight, and the severity of seedling blight was related to the degree of stem rot. To our knowledge, there has been no report that *ZmSBR1* conferred resistance to seedling blight and stem rot caused by *F. verticillioides*. Therefore, this study provides a deeper understanding of the functions of the SAP30_Sin3_bdg motif in plant disease defense. We speculate that *ZmSBR1* confers broad-spectrum, durable resistance to Fusarium diseases at the seedling and adult stages, at least to *F. verticillioides* and *F. graminearum*. It has been reported that genes mediating stem rot resistance may also affect the growth and development of plants, such as regulating the flowering time of maize [54]. However, this study did not investigate the plant height and flowering time of maize at maturity. Therefore, in addition to the role of *ZmSBR1* in stem rot resistance, its effects on flowering time needs to be further explored.

We identified two haplotypes from candidate gene association analysis. After inoculation, inbred lines containing haplotype 1 (CTTGA) reduced the disease grade by about 0.5 compared with those containing haplotype 2 (TCCAG) (Fig. 4B). Analysis of genetic groups revealed that the proportion of disease-resistant haplotypes in inbred lines was less than one-half indicating that most inbred and potential parents of hybrids could benefit from an increased frequency of haplotype 1. The high-quality hybrid models in China are mainly based on Reid × TSPT and Reid × Lancaster combinations. In breeding, P-group and CML materials, which are conducive to improving the disease resistance of maize at the adult stage as donor parent, are generally used to improve the disease resistance of the Reid group. However, based on our results, this disease resistance strategy may not fully apply to seedling blight. The proportion of resistant haplotypes in Reid and Lancaster was 50% and 29%, respectively, but only 6% in TSPT (Fig. 4C). Therefore, we can consider using backcross breeding to improve the seedling blight resistance levels in the Lancaster and TSPT groups. Since *ZmSBR1* not only confers resistance to seedling blight and stalk rot caused by *F. verticillioides* at the seedling stage but also confers resistance to stalk rot caused by *F. graminearum* at the adult stage, we believe that this gene will have a future role in maize disease resistance breeding.

CRediT authorship contribution statement

Yunxia Song: Investigation, Formal analysis, Visualization, Writing – original draft. **Peipei Ma:** Investigation. **Jingyang Gao:** Visualization. **Chaopei Dong:** Investigation. **Zhao Wang:** Investigation. **Yifan Luan:** Formal analysis. **Jiafa Chen:** Conceptualization, Resources, Supervision. **Doudou Sun:** Writing – review & editing. **Pei Jing:** Supervision. **Xuecai Zhang:** Resources. **Weibin Song:** Resources. **Zijian Zhou:** Conceptualization, Formal analysis, Writing – review & editing, Supervision. **Jianyu Wu:** Conceptualization, Writing – review & editing, Supervision, Funding acquisition.

Declaration of competing interest

The authors declare that they have no known competing financial interests or personal relationships that could have appeared to influence the work reported in this paper.

Acknowledgments

We thank Dr. Xiaoduo Lu (Qilu Normal University) and Dr. Chunyi Zhang (Biotechnology Research Institute, CAAS) for providing maize B73 mutant. This work was supported by grants from the National Key Research and Development Program Project of China (2022YFD1201803), and Research on Resistance Genetics of Maize Root Rot Disease, State Key Laboratory of Agronomy College, Henan Agricultural University, China (39990073/111).

Appendix A. Supplementary data

Supplementary data for this article can be found online at https://doi.org/10.1016/j.cj.2024.05.003.

References

[1] A.M. Omori, E.Y.S. Ono, J.G. Bordini, M.T. Hirozawa, M.H.P. Fungaro, M.A. Ono, Detection of *Fusarium verticillioides* by PCR-ELISA based on FUM21 gene, Food Microbiol. 73 (2018) 160–167.
[2] M. Ju, Z. Zhou, C. Mu, X. Zhang, J. Gao, Y. Liang, J. Chen, Y. Wu, X. Li, S. Wang, J. Wen, L. Yang, J. Wu, Dissecting the genetic architecture of *Fusarium verticillioides* seed rot resistance in maize by combining QTL mapping and genome-wide association analysis, Sci. Rep. 7 (2017) 46446.
[3] A. Lanubile, L. Pasini, A. Marocco, Differential gene expression in kernels and silks of maize lines with contrasting levels of ear rot resistance after *Fusarium verticillioides* infection, J. Plant Physiol. 167 (2010) 1398–1406.
[4] Y. Liu, G. Hu, A. Zhang, A. Loladze, Y. Hu, H. Wang, J. Qu, X. Zhang, M. Olsen, F. San Vicente, J. Crossaet, F. Lin, B.M. Prasanna, Genome-wide association study and genomic prediction of Fusarium ear rot resistance in tropical maize germplasm, Crop J. 9 (2021) 325–341.
[5] P. Ma, H. Li, E. Liu, K. He, Y. Song, C. Dong, Z. Wang, X. Zhang, Z. Zhou, Y. Xu, J. Wu, H. Zhang, Evaluation and identification of resistance lines and QTLs of maize to seedborne *Fusarium verticillioides*, Plant Dis. 106 (2022) 2066–2073.
[6] L. Stagnati, A. Lanubile, L.F. Samayoa, M. Bragalanti, P. Giorni, M. Busconi, J.B. Holland, A. Marocco, A genome wide association study reveals markers and genes associated with resistance to *Fusarium verticillioides* infection of seedlings in a maize diversity panel, G3-Genes Genomes Genet. 9 (2019) 571–579.
[7] L. Wu, X. Wang, R. Xu, H. Li, Difference between resistant and susceptible maize to systematic colonization as revealed by DsRed-labeled *Fusarium verticillioides*, Crop J. (2013) 61–69.
[8] Y. Xu, Z. Zhang, P. Lu, R. Li, P. Ma, J. Wu, T. Li, H. Zhang, Increasing *Fusarium verticillioides* resistance in maize by genomics-assisted breeding: methods, progress, and prospects, Crop J. 11 (2023) 1626–1641.
[9] C.W. Bacon, D.M. Hinton, Fusaric acid and pathogenic interactions of corn and non-corn isolates of *Fusarium moniliforme*, a nonobligate pathogen of corn, Adv. Exp. Med. Biol. 392 (1996) 175–191.
[10] C.G. Afolabi, P.S. Ojiambo, E.J.A. Ekpo, A. Menkir, R. Bandyopadhyay, Novel sources of resistance to Fusarium stalk rot of maize in tropical Africa, Plant Dis. 92 (2008) 772–780.
[11] T.T. Baldwin, N.C. Zitomer, T.R. Mitchell, A.M. Zimeri, C.W. Bacon, R.T. Riley, A. E. Glenn, Maize seedling blight induced by *Fusarium verticillioides*: accumulation of fumonisin B_1 in leaves without colonization of the leaves, J. Agric. Food. Chem. 62 (2014) 2118–2125.
[12] A.E. Glenn, N.C. Zitomer, A.M. Zimeri, L.D. Williams, R.T. Riley, R.H. Proctor, Transformation-mediated complementation of a FUM gene cluster deletion in *Fusarium verticillioides* restores both fumonisin production and pathogenicity on maize seedlings, Mol. Plant-Microbe Interact. 21 (2008) 87–97.
[13] L.D. Williams, A.E. Glenn, C.W. Bacon, M.A. Smith, R.T. Riley, Fumonisin production and bioavailability to maize seedlings grown from seeds inoculated with *Fusarium verticillioides* and grown in natural soils, J. Agric. Food Chem. 54 (2006) 5694–5700.
[14] T.M. Tran, M. Ameye, F. Devlieghere, S. De Saeger, M. Eeckhout, K. Audenaert, *Streptomyces* strains promote plant growth and induce resistance against *Fusarium verticillioides* via transient regulation of auxin signaling and archetypal defense pathways in maize plants, Front. Plant Sci. 12 (2021) 755733.
[15] P. Septiani, A. Lanubile, L. Stagnati, M. Busconi, H. Nelissen, M.E. Pè, M. Dell'Acqua, A. Marocco, Unravelling the genetic basis of Fusarium seedling rot resistance in the MAGIC maize population: novel targets for breeding, Sci. Rep. 9 (2019) 5665.
[16] A. Lanubile, V.M.G. Borrelli, M. Soccio, P. Giorni, L. Stagnati, M. Busconi, A. Marocco, Loss of ZmLIPOXYGENASE4 decreases *Fusarium verticillioides* resistance in maize seedlings, Genes (basel) 12 (2021) 335.
[17] S.A. Christensen, A. Nemchenko, Y.S. Park, E. Borrego, P.C. Huang, E.A. Schmelz, S. Kunze, I. Feussner, N. Yalpani, R. Meeley, M.V. Kolomiets, The novel monocot-specific 9-lipoxygenase ZmLOX12 is required to mount an effective jasmonate-mediated defense against *Fusarium verticillioides* in maize, Mol. Plant-Microbe Interact. 27 (2014) 1263–1276.

[18] H. Dong, P. Qin, Z. Gao, J. Xu, X. Xu, First report of seedling blight of maize caused by *Fusarium asiaticum* in northeast China, Plant Dis. 4 (2020) 1206.
[19] Y. Sun, X. Ruan, L. Ma, F. Wang, X. Gao, Rapid screening and evaluation of maize seedling resistance to stalk rot caused by *Fusarium* spp., Bio-Protocol 8 (2018) e2859.
[20] P. Ma, E. Liu, Z. Zhang, T. Li, Z. Zhou, W. Yao, J. Chen, J. Wu, Y. Xu, H. Zhang, Genetic variation in *ZmWAX2* confers maize resistance to *Fusarium verticillioides*, Plant Biotechnol. J. 21 (2023) 1812–1826.
[21] L. Li, Q. Qu, Z. Cao, Z. Guo, H. Jia, N. Liu, Y. Wang, J. Dong, The relationship analysis on corn stalk rot and ear rot according to *Fusarium* species and Fumonisin contamination in kernels, Toxins (basel) 11 (2019) 320.
[22] J. Ren, X. Wu, X. Sun, A study on infection cycle of pathogen of corn ear rot and stalk rot in Jilin province, Maize Sci. 3 (1995) 25–28.
[23] X. Gai, H. Dong, S. Wang, B. Liu, Z. Zhang, X. Li, Z. Gao, Infection cycle of maize stalk rot and ear rot caused by *Fusarium verticillioides*, PLoS ONE 13 (2018) e0201588.
[24] S. Wang, W. Liu, Z. Chen, J. Zhang, X. Jia, M. Gou, X. Chen, Y. Zhang, H. Li, Y. Chen, The antioxidant protein ZmPrx5 contributes resistance to maize stalk rot, Crop J. 10 (2022) 1049–1058.
[25] J. Ding, L. Zhang, J. Chen, X. Li, Y. Li, H. Cheng, R. Huang, B. Zhou, Z. Li, J. Wang, J. Wu, Genomic dissection of leaf angle in maize (*Zea mays* L.) using a four-way cross mapping population, PLoS ONE 10 (2015) e0141619.
[26] R.J. Elshire, J.C. Glaubitz, Q. Sun, J.A. Poland, K. Kawamoto, E.S. Buckler, S.E. Mitchell, A robust, simple genotyping-by-sequencing (GBS) approach for high diversity species, PLoS ONE 6 (2011) e19379.
[27] X. Li, Z. Zhou, J. Ding, Y. Wu, B. Zhou, R. Wang, J. Ma, S. Wang, X. Zhang, Z. Xia, J. Chen, J. Wu, Combined linkage and association mapping reveals QTL and candidate genes for plant and ear height in maize, Front. Plant Sci. 7 (2016) 833.
[28] J. Gao, S. Wang, Z. Zhou, S. Wang, C. Dong, C. Mu, Y. Song, P. Ma, C. Li, Z. Wang, K. He, C. Han, J. Chen, H. Yu, J. Wu, Linkage mapping and genome-wide association reveal candidate genes conferring thermotolerance of seed-set in maize, J. Exp. Bot. 70 (2019) 4849–4864.
[29] C. Mu, J. Gao, Z. Zhou, Z. Wang, X. Sun, X. Zhang, H. Dong, Y. Han, X. Li, Y. Wu, Y. Song, P. Ma, C. Dong, J. Chen, J. Wu, Genetic analysis of cob resistance to *F. verticillioides*: another step towards the protection of maize from ear rot, Theor. Appl. Genet. 132 (2019) 1049–1059.
[30] M. Li, Y. Zhang, Z. Zhang, Y. Xiang, M. Liu, Y. Zhou, J. Zuo, H. Zhang, Y. Chen, Y. Zhang, A compressed variance component mixed model for detecting QTNs and QTN-by-environment and QTN-by-QTN interactions in genome-wide association studies, Mol. Plant 15 (2022) 630–650.
[31] M. Li, Y. Zhang, Y. Xiang, M. Liu, Y. Zhang, IIIVmrMLM: The R and C++ tools associated with 3VmrMLM, a comprehensive GWAS method for dissecting quantitative traits, Mol. Plant 15 (2022) 1251–1253.
[32] F. He, S. Ding, H. Wang, F. Qin, IntAssoPlot: An R package for integrated visualization of genome-wide association study results with gene structure and linkage disequilibrium matrix, Front. Genet. 11 (2020) 260.
[33] C. Chen, H. Chen, Y. Zhang, H.R. Thomas, M.H. Frank, Y. He, R. Xia, TBtools: an integrative toolkit developed for interactive analyses of big biological data, Mol. Plant 13 (2020) 1194–1202.
[34] X. Lu, J. Liu, W. Ren, Q. Yang, Z. Chai, R. Chen, L. Wang, J. Zhao, Z. Lang, H. Wang, Y. Fan, J. Zhao, C. Zhan, Gene-indexed mutations in maize, Mol. Plant 11 (2018) 496–504.
[35] S.N. Gangappa, J.F. Botto, The multifaceted roles of HY5 in plant growth and development, Mol. Plant 9 (2016) 1353–1365.
[36] Q. He, H. Cai, M. Bai, M. Zhang, F. Chen, Y. Huang, S. Priyadarshani, M. Chai, L. Liu, Y. Liu, H. Chen, Y. Qin, A soybean bZIP transcription factor GmbZIP19 confers multiple biotic and abiotic stress responses in plants, Int. J. Mol. Sci. 21 (2020) 4701.
[37] H. Ma, C. Liu, Z. Li, Q. Ran, G. Xie, B. Wang, S. Fang, J. Chu, J. Zhang, *ZmbZIP4* contributes to stress resistance in maize by regulating ABA synthesis and root development, Plant Physiol. 178 (2018) 753–770.
[38] P. Sornaraj, S. Luang, S. Lopato, M. Hrmova, Basic leucine zipper (bZIP) transcription factors involved in abiotic stresses: a molecular model of a wheat bZIP factor and implications of its structure in function, Biochim. Biophys. Acta 2016 (1860) 46–56.
[39] B. Qu, Z. Ma, L. Yao, Z. Gao, S. Zhang, Preserved antibacterial activity of ribosomal protein S15 during evolution, Mol. Immunol. 127 (2020) 57–66.
[40] N. Bollier, N. Gonzalez, C. Chevalier, M. Hernould, Zinc finger-homeodomain and mini zinc finger proteins are key players in plant growth and responses to environmental stresses, J. Exp. Bot. 73 (2022) 4662–4673.
[41] J.C. Jang, Arginine-rich motif-tandem CCCH zinc finger proteins in plant stress responses and post-transcriptional regulation of gene expression, Plant Sci. 252 (2016) 118–124.
[42] H. Zhang, T. Zhao, P. Zhuang, Z. Song, H. Du, Z. Tang, Z. Gao, NbCZF1, a novel C2H2-type zinc finger protein, as a new regulator of SsCut-induced plant immunity in *Nicotiana benthamiana*, Plant Cell Physiol. 57 (2016) 2472–2484.
[43] G. de Jong, A.K.A. Pamplona, R.G. Von Pinho, M. Balestre, Genome-wide association analysis of ear rot resistance caused by *Fusarium verticillioides* in maize, Genomics 5 (2018) 291–303.
[44] L.F. Samayoa, A. Cao, R. Santiago, R.A. Malvar, A. Butrón, Genome-wide association analysis for fumonisin content in maize kernels, BMC Plant Biol. 19 (2019) 166.
[45] L. Stagnati, V. Rahjoo, L.F. Samayoa, J.B. Holland, V.M.G. Borrelli, M. Busconi, A. Lanubile, A. Marocco, A genome-wide association study to understand the effect of Fusarium verticillioides infection on seedlings of a maize diversity panel, G3-Genes Genomes Genet. 10 (2020) 1685–1696.
[46] Y. Zhang, Z.W. Sun, R. Iratni, H. Erdjument-Bromage, P. Tempst, M. Hampsey, D. Reinberg, SAP30, a novel protein conserved between human and yeast, is a component of a histone deacetylase complex, Mol. Cell 1 (1998) 1021–1031.
[47] C.D. Laherty, A.N. Billin, R.M. Lavinsky, G.S. Yochum, A.C. Bush, J.M. Sun, T.M. Mullen, J.R. Davie, D.W. Rose, C.K. Glass, M.G. Rosenfeld, D.E. Ayer, R.N. Eisenman, SAP30, a component of the mSin3 corepressor complex involved in N-CoR-mediated repression by specific transcription factors, Mol. Cell 2 (1998) 33–42.
[48] H.G. Lee, C. Hong, P.J. Seo, The Arabidopsis Sin3-HDAC complex facilitates temporal histone deacetylation at the CCA1 and PRR9 loci for robust circadian oscillation, Front. Plant Sci. 10 (2019) 171.
[49] X. Liu, S. Yang, M. Zhao, M. Luo, C.W. Yu, C.Y. Chen, R. Tai, K. Wu, Transcriptional repression by histone deacetylases in plants, Mol. Plant 7 (2014) 764–772.
[50] X. Ma, S. Lv, C. Zhang, C. Yang, Histone deacetylases and their functions in plants, Plant Cell Rep. 32 (2013) 465–478.
[51] M.S. Tahir, L. Tian, HD2-type histone deacetylases: unique regulators of plant development and stress responses, Plant Cell Rep. 40 (2021) 1603–1615.
[52] M. Tiana, B. Acosta-Iborra, L. Puente-Santamaría, P. Hernansanz-Agustin, R. Worsley-Hunt, N. Masson, F. García-Rio, D. Mole, P. Ratcliffe, W.W. Wasserman, B. Jimenez, L.D. Peso, The SIN3A histone deacetylase complex is required for a complete transcriptional response to hypoxia, Nucleic Acids Res. 46 (2018) 120–133.
[53] K.M. Viiri, H. Korkeamäki, M.K. Kukkonen, L.K. Nieminen, K. Lindfors, P. Peterson, M. Mäki, H. Kainulainen, O. Lohi, SAP30L interacts with members of the Sin3A corepressor complex and targets Sin3A to the nucleolus, Nucleic Acids Res. 34 (2006) 3288–3298.
[54] H. Su, J. Lian, S.F. Abou-Elwafa, H. Cheng, D. Dou, Z. Ren, J. Xie, Z. Chen, F. Gao, L. Ku, Y. Chen, *ZmCCT* regulates photoperiod-dependent flowering and response to stresses in maize, BMC Plant Biol. 21 (2021) 453.